Street Heating: Modeling for Control

Bernt Lie
Telemark University College, Porsgrunn, Norway

August 21, 2013

Abstract

The study deals with the possibility of reducing peak power consumption when melting snow/ice on pavements, by including meteorological prediction models. It is shown that if meteorological predictions are reasonably accurate e.g. more than 5 h into the future, the use of expensive fossil/electrical back-up fuel can be reduced in district heating systems based on bio fuel.

1 Introduction

The removal of snow from roads, streets, plazas, etc. is a considerable cost to society in Northern countries. The use of plows has been partially replaced by the use of salt, but salt has negative impact wrt. corrosion and on the environment. During the last 2-3 decades, the infrastructure of cities in Norway has changed e.g. with the building of compact residential areas surrounding plazas with cobbled stone, etc.; plows are thus often unsuitable for the removal of snow/ice, and the installation of street heating is a viable alternative.

Street heating is part of district heating systems, where the energy may be surplus hot water from industry, or water heated using fossil fuel, electricity, biomass, etc. Although Norway is in a special situation with 98% of the electricity production (120TWh) based on low cost hydro power, and a considerable use of electricity for heating buildings (45TWh), there is also a substantial annual growth of biomass of $25 \times 10^6\,\mathrm{m}^3$ where less than half of it is currently used (buildings, paper industry, heating). Because electricity can be exported at a high price, biomass is a less expensive power source in district heating than electricity or fossil fuel.

With the latent heat involved in melting snow/ice, the requirement to keep streets snow/ice free, and the considerable time constants in heating the ground, this traditionally leads to extreme peaks in the power consumption during precipitation, with the need to use expensive electricity or fossil fuel in addition to biofuel. It is thus of interest to consider the following: is it possible to use meteorological models for predicting precipitation of ice/snow, and combine this with dynamic models for pre-heating the ground/street before the precipitation takes place, and this way avoid using costly back-up fuels? Ensembles of meteorological predictions are readily available from meteorological institutes[1]. These predictions may need to be extended with e.g. radiation predictions. Models of the ground are used in design studies within civil engineering; Lyseng (2012) gives a description for a case study in Notodden, Norway. Models of the build-up of snow/ice above the ground has been studied in some detail e.g. in a number of studies at Oklahoma State University (Liu, 2005); see also e.g. Chen *et al.* (2011) and Wang *et al.* (2010).

In this study, a model of the ground is used in conjunction with a simple model of ice accumulation to indicate how meteorological predictions can aid in reducing the energy costs in street heating. The paper is organized as follows. In section 2, a functional system description is given. In section 3, a dynamic model is given. In section 4, operational studies illustrate how

[1] See e.g. `www.storm.no`.

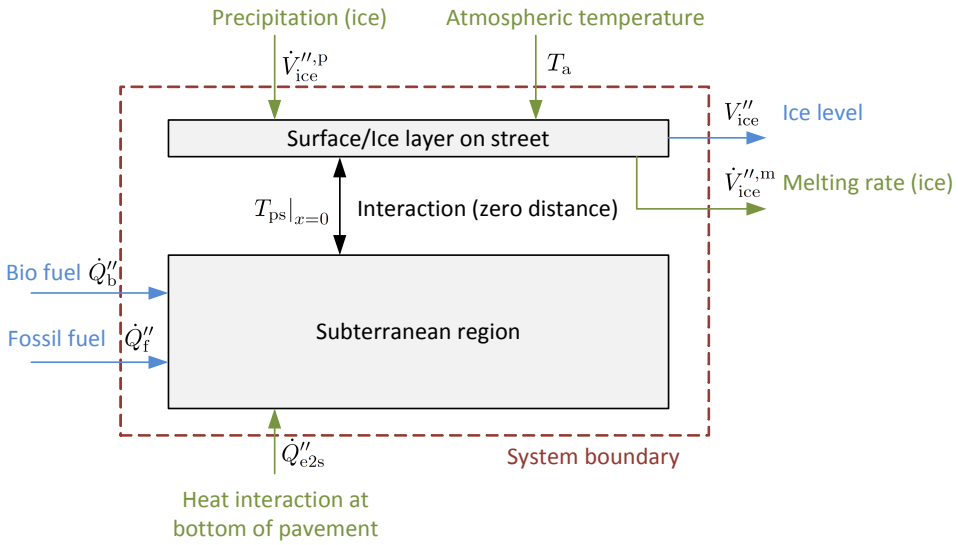

Figure 1: Functional description of street heating system, with control inputs (blue), disturbances (green), and controlled variable (blue).

prior knowledge of precipitation can be used to avoid the use of costly back-up fuel. In section 5, some conclusions are drawn.

2 System description

2.1 Functional description

Figure 1 illustrates the inputs to the system: control inputs $\dot{Q}''_{\mathrm{b}}$ (bio fuel heat flow per area), $\dot{Q}''_{\mathrm{f}}$ (fossil fuel heat flow per area), and disturbance $\dot{V}''^{,\mathrm{p}}_{\mathrm{ice}}$ (volumetric precipitation rate per area), $\dot{V}''^{,\mathrm{m}}_{\mathrm{ice}}$ (melting rate of ice), T_{a} (atmospheric temperature), and $\dot{Q}''_{\mathrm{e2s}}$ (interaction with inner earth), as well as the controlled variable V''_{ice} (ice volume per area = ice level). In addition, there ice interactionbetween the subterranean region and the ice layer.

The main control problem is to remove the ice layer, i.e. reduce V''_{ice} to zero by using the control inputs. Both heat inputs $\dot{Q}''_{\mathrm{b}}$ and $\dot{Q}''_{\mathrm{f}}$ are constrained and the expensive fossil fuel should be avoided, i.e. $\dot{Q}''_{\mathrm{f}}$ should rather not be used. The precipitation rate $\dot{V}''^{,\mathrm{p}}_{\mathrm{ice}}$ is a disturbance which may be possible to predict using meteorology. The interaction with inner earth, disturbance $\dot{Q}''_{\mathrm{e2s}}$, is modeled, together with the melting rate. Atmospheric temperature influences the subterranean region when the surface is ice-free.

In a more extensive study, it may be relevant to accept an ice layer if the atmospheric temperature is sufficiently low to avoid slippery conditions, but this case will not be considered here.

2.2 Geometric layout

Figure 2 illustrates the pavement layout as suggested in Lyseng (2012). The pavement consists of a top layer of paving stones, followed by sand, an upper asphalt layer with glycol pipes, a lower asphalt layer, a layer of small crushed stones, and a layer of large crushed stones. Below the pavement is assumed to be soil. The relative thicknesses of the various layers in the pavement is approximately as indicated in fig. 2.

Heat is transported into the pavement from the district heating system via a heat exchanger to a glycol circuit, and the glycol pipes typically have a snake-like shape in the asphalt layer[2];

[2] See `www.wattsradiant.com`.

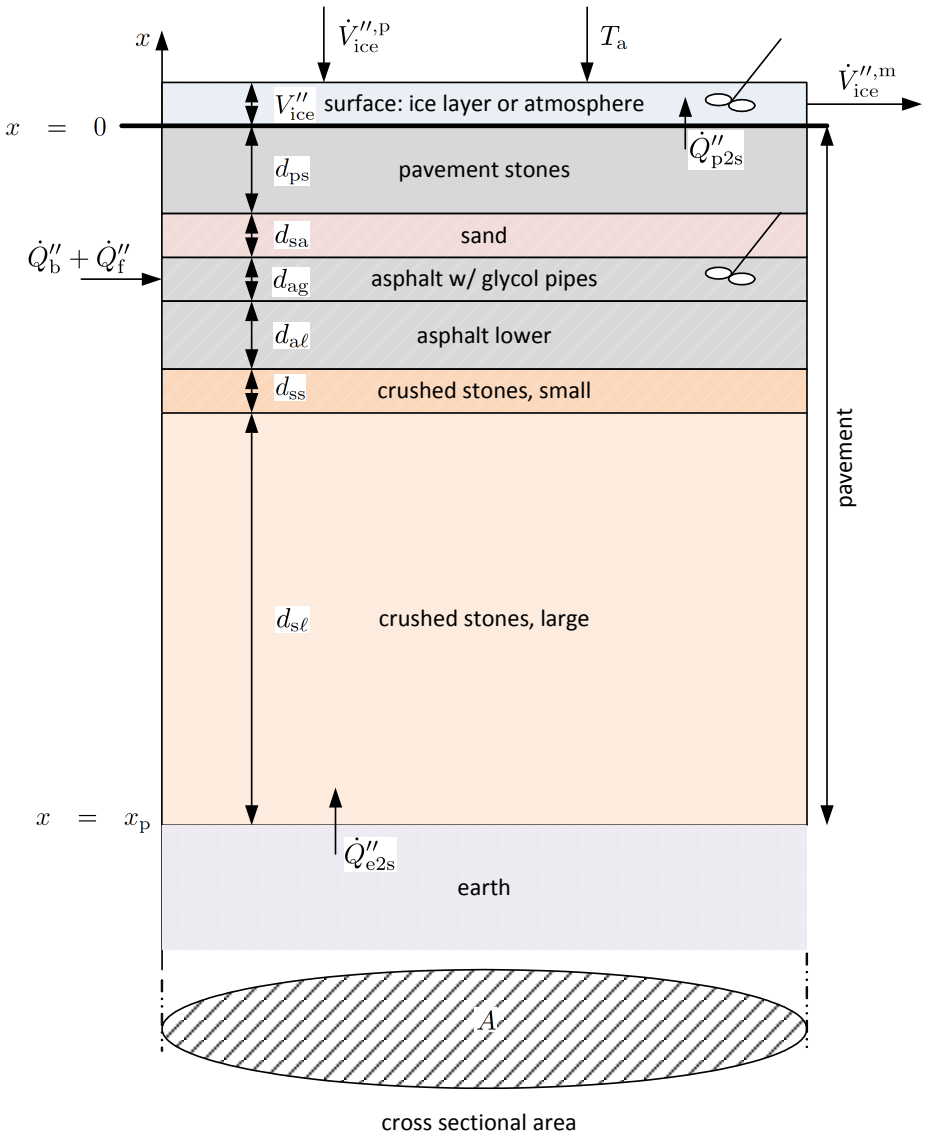

Figure 2: Geometric layout of pavement for street heating, with approximately real ratios of layer thicknesses. After Lyseng (2012).

for simplicity it may be assumed that the glycol circuit leads to a homogeneous temperature in the upper asphalt layer. Furthermore, the dynamics of the glycol circuit is neglected, and it is assumed that the heat from the biofuel and the fossil fuel is transported directly into the upper asphalt layer.

3 Dynamic model

3.1 Principles

In the model, we will assume perfectly homogeneous conditions horisontally over the cross sectional area A (fig. 2), but variations in the vertical direction (x-axis). In reality, there will be variations in the cross sectional area too (Chen *et al.*, 2011), but we will not have sufficient detailed information about precipitation and will thus neglect this variation.

Several layers share the same equations, and it is convenient to define model classes. Such classes should only contain material property information for the subsystem in question, and any properties in neighbor subsystems should be transferred through input signals.

A key property of the system is that no energy is accumulated at the interphases between the layers, thus the heat flow that flows out of a layer must also flow into the neighbor layer. Furthermore, when discretizing the layers in space with control volume thickness Δx, the temperature must be continuous when $\Delta x \to 0$ — except at interphases with heat conduction/convection, where there is a jump in the temperature.

3.2 Asphalt layer with glycol pipes

The asphalt layer with glycol pipes could be divided into the asphalt volume and the glycol pipes with heat exchanger connecting it to the district heating system. However, the dynamics of the glycol pipes will probably be much faster than that of the rest of the system, so here a simplified description with direct input of bio fuel and fossil heat flux into the asphalt volume is considered, see Appendix **??**.

Assuming a well mixed asphalt volume in the layer with asphalt and glycol pipes, this leads to the model

$$\frac{dT_{\mathrm{a1}}}{dt} = \frac{\dot{Q}''_{\mathrm{b}} + \dot{Q}''_{\mathrm{f}} + \dot{Q}''_{\mathrm{a2a}} - \dot{Q}''_{\mathrm{a2s}}}{\rho_{\mathrm{a}} d_{\mathrm{ag}} \hat{c}_{\mathrm{p,a}}}$$

where ρ_{a} is the asphalt density, d_{a1} is the thickness of the upper asphalt layer[3], $\hat{c}_{\mathrm{p,a}}$ is the specific heat capacity of asphalt, $\dot{Q}''_{\mathrm{b}}$ and $\dot{Q}''_{\mathrm{f}}$ are the heat fluxes of bio fuel and fossil fuel, respectively, $\dot{Q}''_{\mathrm{a2a}}$ is the upward heat flux between the asphalt layers, and $\dot{Q}''_{\mathrm{a2s}}$ is the upward heat flux from the upper asphalt layer to the sand layer.

With the assumption of continuous temperature in the solid layers and no energy accumulation at the interfaces, it follows that

$$\begin{aligned} \dot{Q}''_{\mathrm{a2a}} &= \dot{Q}''^{,\mathrm{a}\ell}_{N_{\mathrm{a}\ell}} = -k_{\mathrm{a}} \frac{T_{\mathrm{a1}} - T^{\mathrm{a}\ell}_{N_{\mathrm{a}\ell}}}{\Delta x_{\mathrm{a}\ell}} \\ \dot{Q}''_{\mathrm{a2s}} &= \dot{Q}''^{,\mathrm{sa}}_{0} = -k_{\mathrm{a}} \frac{T^{\mathrm{sa}}_{1} - T_{\mathrm{ag}}}{\Delta x_{\mathrm{sa}}}. \end{aligned}$$

The class is illustrated in fig. 3, where $\dot{Q}''_{\ell} = \dot{Q}''_{\mathrm{a2a}}$ and $\dot{Q}''_{\mathrm{u}} = \dot{Q}''_{\mathrm{a2s}}$.

[3] Some correction should probably be made to compensate for the fact that the asphalt layer contains both asphalt and glycol pipes.

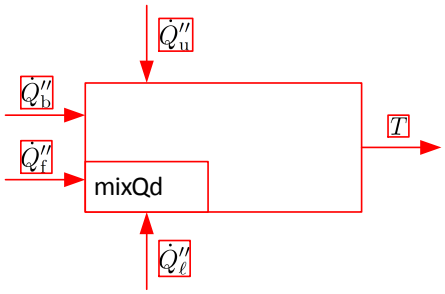

Figure 3: Class of perfectly mixed volume with heat inputs $\dot{Q}''_{\mathrm{b}}$, $\dot{Q}''_{\mathrm{f}}$, $\dot{Q}''_{\mathrm{u}}$, $\dot{Q}''_{\ell}$.

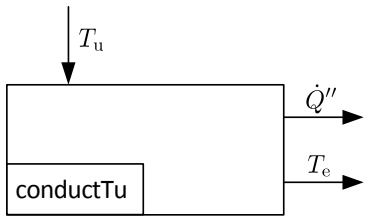

Figure 4: Earth class for heat conduction with input upper temperature T_{u}.

3.3 Earth below pavement

The heat flow $\dot{Q}''_{\mathrm{e2s}}$ from the earth below the pavement and into the large crushed stone layer is assumed to be given by

$$\dot{Q}''_{\mathrm{e2s}} = U_{\mathrm{e2s}} \left(T_{\mathrm{e}} - T_1^{\mathrm{sl}} \right)$$

where U_{e2s} is some overall heat transfer coefficient, T_{e} is the earth temperature below the pavement, and T_1^{sl} is the bottom temperature in the large crushed stone layer. Alternative descriptions are possible. A common experience is that in the interval $[15, 40]$ m below the surface, the earth temperature is constant and equal to the annual average atmospheric temperature of the location. Clearly, a street heating system may alter this experience somewhat.

Figure 4 illustrates the structure of this class.Thus, $T_{\mathrm{u}} = T_1^{\mathrm{s}\ell}$, and $\dot{Q}'' = \dot{Q}''_{\mathrm{e2s}}$.

3.4 Surface

3.4.1 Atmosphere

If the surface is ice-free, $V''_{\mathrm{ice}} = 0$, and the heat transfer to the surface is

$$\dot{Q}''_{\mathrm{p2s}} = h_{\mathrm{p2a}} \left(T_{N_{\mathrm{ps}}}^{\mathrm{ps}} - T_{\mathrm{a}} \right)$$

where h_{p2a} is the heat transfer coefficient to (moving) air, $T_{N_{\mathrm{ps}}}^{\mathrm{ps}}$ is the surface temperature of the pavement stones and T_{a} is the atmospheric temperature. In reality, radiation will also play a role, but this is neglected in this study: the inclusion of radiation is relatively straight forward, but includes some fuzzy details such as cloud temperature.

3.4.2 Ice layer

By assuming constant ice density, a model of the ice layer V''_{ice} (ice volume per area A = ice level) becomes

$$\frac{dV''_{\mathrm{ice}}}{dt} = \dot{V}''^{,\mathrm{p}}_{\mathrm{ice}} - \dot{V}''^{,\mathrm{m}}_{\mathrm{ice}}$$

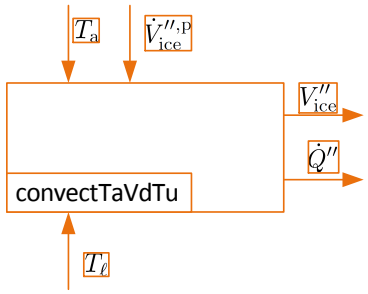

Figure 5: Surface class with heat convection and inputs precipitation $\dot{V}''^{,p}_{ice}$, atmospheric temperature T_a, and lower temperature T_ℓ.

where $\dot{V}''^{,p}_{ice}$ is volumetric rate per area A (unit: length/time, e.g. precipitation $\dot{V}''^{,p}_{ice}$ may have unit mm/ h) and

$$\dot{V}''^{,m}_{ice} \approx \frac{\dot{Q}''_{p2s}}{\rho_{ice}\Delta\hat{H}^{m}_{ice}}$$

and ρ_{ice} is the density of ice and $\Delta\hat{H}^{m}_{ice}$ is the specific enthalpy of melting for ice. $\dot{Q}''_{p2s}$ is the heat flow from the pavement to the surface/the ice.

The heat transfer between the surface of the pavement stones and the melting ice is given by heat transfer to melted water:

$$\dot{Q}''_{p2s} = h_{p2w}\left(T^{ps}_{N_{ps}} - T^{m}_{w}\right)$$

where $T^{m}_{w} = 0\,°C$.

Figure 5 illustrates the structure of this class.Here, $T_\ell = T^{ps}_{N_{ps}}$.

3.5 Temperature distribution in layers

3.5.1 Heat diffusion

Dynamic heat diffusion is considered in all layers of fig. 2, except the surface layer, the earth layer, and the upper asphalt layer which includes the glycol pipes. A standard heat diffusion model is suggested:

$$\frac{\partial T}{\partial t} = -\frac{1}{\rho\hat{c}_p}\frac{\partial\dot{Q}''}{\partial x}$$

where $T = T(t, x)$ is the temperature distribution, t is time, x is vertical position, ρ is density, $\hat{c}_p$ is specific heat capacity, and $\dot{Q}''$ is heat flux (heat flow per unit area). The heat flux is given by Fourier's equation:

$$\dot{Q}'' = -k\frac{\partial T}{\partial x}$$

where k is heat conductivity.

3.5.2 Discretization and boundary conditions

A standard discretization of this model is

$$\begin{aligned}\frac{dT_{x+\Delta x}}{dt} &= -\frac{1}{\rho\hat{c}_p}\frac{\dot{Q}''_{x+\Delta x} - \dot{Q}''_x}{\Delta x}\\ \dot{Q}''_x &= -k\frac{T_{x+\Delta x} - T_x}{\Delta x}\end{aligned}$$

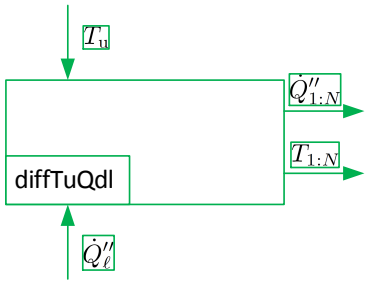

Figure 6: Heat diffusion class with specified upper temperature T_u and lower heat flow $\dot{Q}''_\ell$.

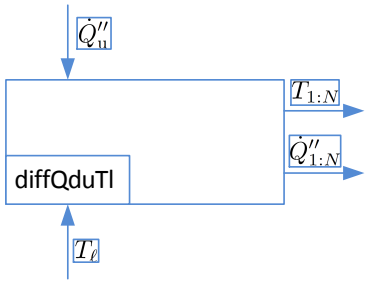

Figure 7: Heat diffusion class with specified upper heat flow $\dot{Q}''_u$ and lower temperature T_ℓ.

where Δx is the thickness of the control volume within the layer, and Δx typically is constant and given as

$$\Delta x = \frac{d}{N}$$

where d is the layer thickness and N is the number of control volumes/slices in the layer.

The structure of general layer classes are illustrated in fig. 6 and fig. 7.

3.6 The total model

The total model structure is displayed in fig. 8; compare fig. 8 with fig. 2.

3.7 Model parameters and operational conditions

Parameters and nominal operational conditions for the model are taken from Lyseng (2012), with minor adjustments.

4 Simulation

4.1 Preliminaries

In all simulations, the time axis is given in hours. Figure 9 illustrates the assumed precipitation $\dot{V}''^{,\mathrm{p}}_{\mathrm{ice}}$ (denoted `sh.oVd_ice_p`) in mm/ h, i.e. 3 mm/ h in the period $[10, 12]$ h.

In the subsequent simulations, the responses in some temperatures and the ice level are computed based on various heating policies. The simulations show the effect of including various numbers of control volumes in the layers; for simplicity, the same number of control volumes are used in every distributed layer. Some of the variables have been scaled from the internal values in the simulator; thus the presented variables are denoted *output* variables. The general notation used is `shNx`, where `sh` implies *street heating*, `N` is the number of control volumes in the layers, and `x` is the presented variable. The presented variable names (`x`) are `oT_a` for atmospheric temperature T_a, `oT_ea` for earth temperature T_e, `oT_ag` for temperature T_{ag} in

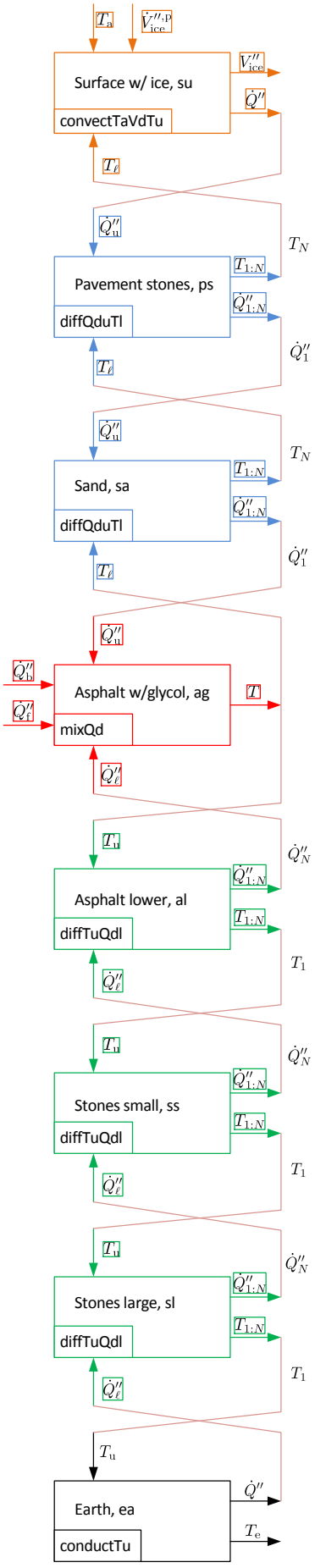

Figure 8: The total model structure, with interaction between instances of the classes.

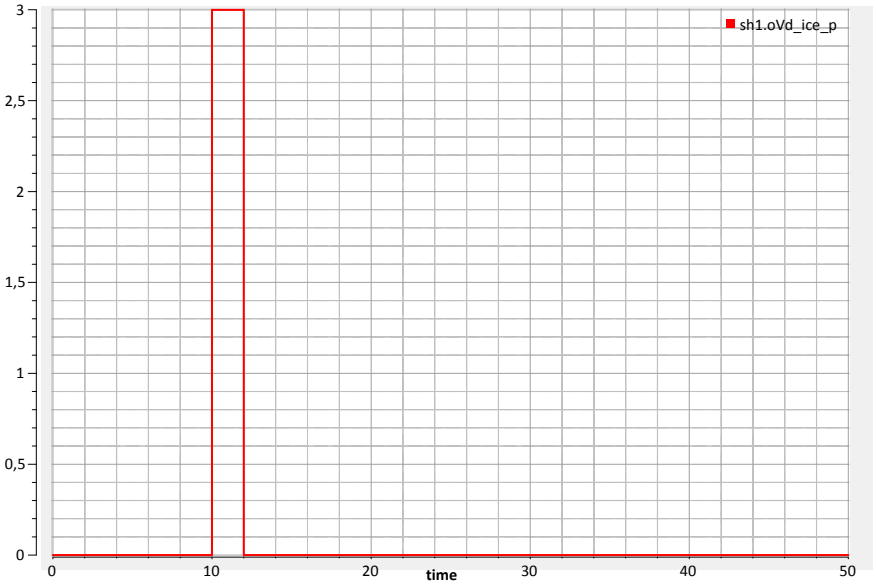

Figure 9: Precipitation of ice, in mm/ h.

the well mixed asphalt layer with glycol pipes,and `oT_su` for the surface temperature of the pavement stones $T_{\mathrm{ps}}|_{x=0}$; all temperatures are given in centigrades. `oV_ice` denotes the ice layer V''_{ice} (mm). The heating policies are denoted `oQd_b` for $\dot{Q}''_{\mathrm{b}}$ (bio fuel, $\mathrm{W/\,m^2}$) and `oQd_f` for $\dot{Q}''_{\mathrm{f}}$ (fossil fuel; $\mathrm{W/\,m^2}$).

In this study, $\dot{Q}''_{\mathrm{b}}$ is assumed to be constrained by $\dot{Q}''_{\mathrm{b}} \leq 50\,\mathrm{W/\,m^2}$. The fossil fuel is constrained by $\dot{Q}''_{\mathrm{f}} \leq 220\,\mathrm{W/\,m^2}$.

4.2 Combined biofuel and fossil fuel heating at onset of precipitation

Figure 10 illustrates the heating profile used with onset of biofuel at 10 h, when the precipitation starts.In the figure, the fossil fuel heating is turned off when the ice layer disappears. The same would be done for bio fuel, but that is not important for the study here.

Figure 11 shows the computed temperature in the (upper) asphalt layer with glycol pipes, and in the surface of the pavement stones for various numbers of control volumes per layer, $N \in \{1, 5, 10, 20, 50\}$.

Figure 12 shows the computed layer of ice on the surface for various numbers of control volumes per layer, $N \in \{1, 5, 10, 20, 50\}$.

4.3 Biofuel heating at onset of precipitation

Figure 13 illustrates the heating profile used with onset of biofuel at 10 h, when the precipitation starts. Figure 14 shows the computed temperature in the upper asphalt layer with glycol pipes, and in the surface of the pavement stones for various numbers of control volumes per layer, $N \in \{1, 5, 10, 20, 50\}$.

Figure 15 shows the computed layer of ice on the surface for various numbers of control volumes per layer, $N \in \{1, 5, 10, 20, 50\}$.

4.4 Biofuel heating with onset infinitely prior to precipitation

Figure 16 illustrates the heating profile used with onset of biofuel at $-\infty$ h.

Figure 17 shows the computed temperature in the upper asphalt layer with glycol pipes, and in the surface of the pavement stones for various numbers of control volumes per layer, $N \in \{1, 5, 10, 20, 50\}$.

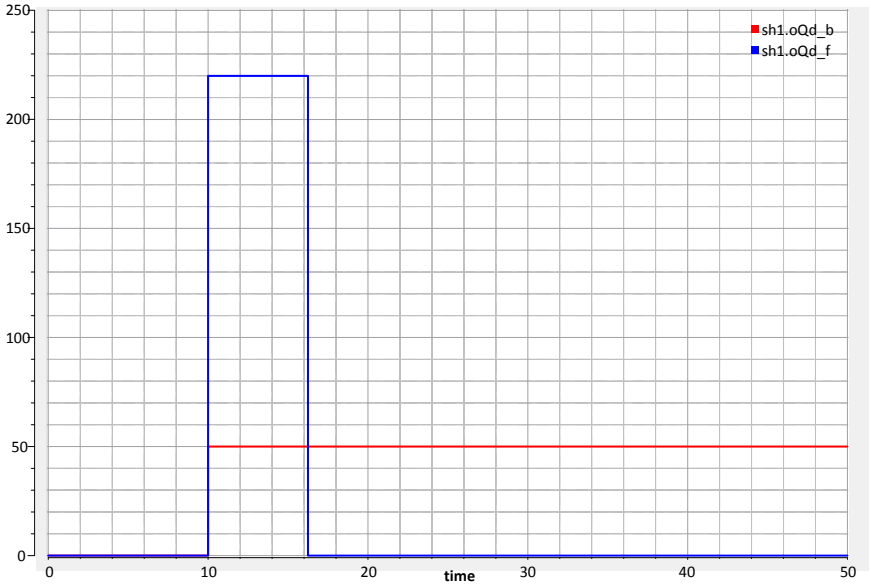

Figure 10: Heating levels, $\dot{Q}''_{\mathrm{b}}$ jumps from $0\,\mathrm{W/m^2}$ to $50\,\mathrm{W/m^2}$ after 10 h, while $\dot{Q}''_{\mathrm{f}}$ jumps to $220\,\mathrm{W/m^2}$ during ice coverage of the surface.

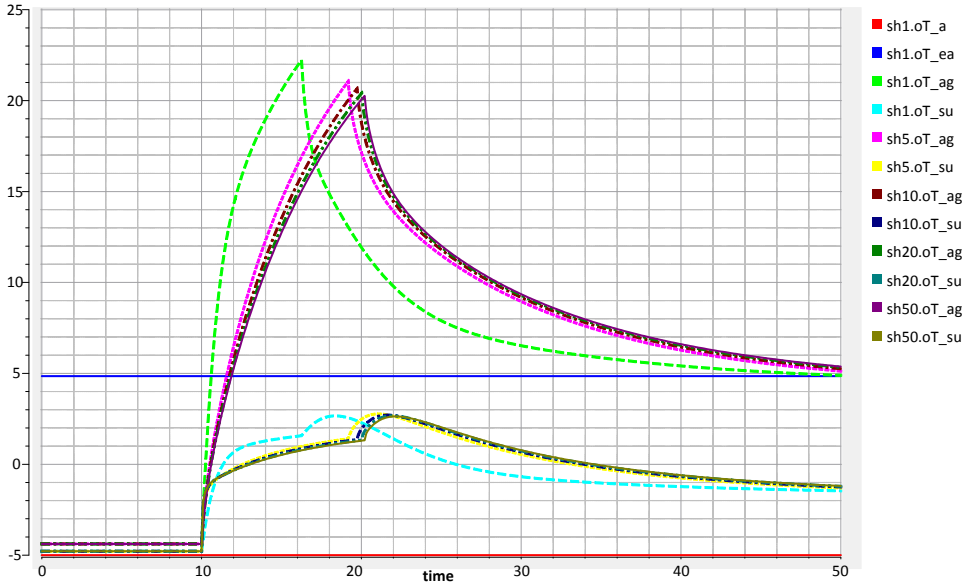

Figure 11: Computed temperature in asphalt layer with glycol pipes (`shN.oT_ag`) and at the surface of the pavement stones (`shN.oT_su`), where `N` specifies the number of control volumes in layers. Atmospheric temperature (`sh1.oT_a`) and earth temperature (`sh1.oT_ea`) are included.

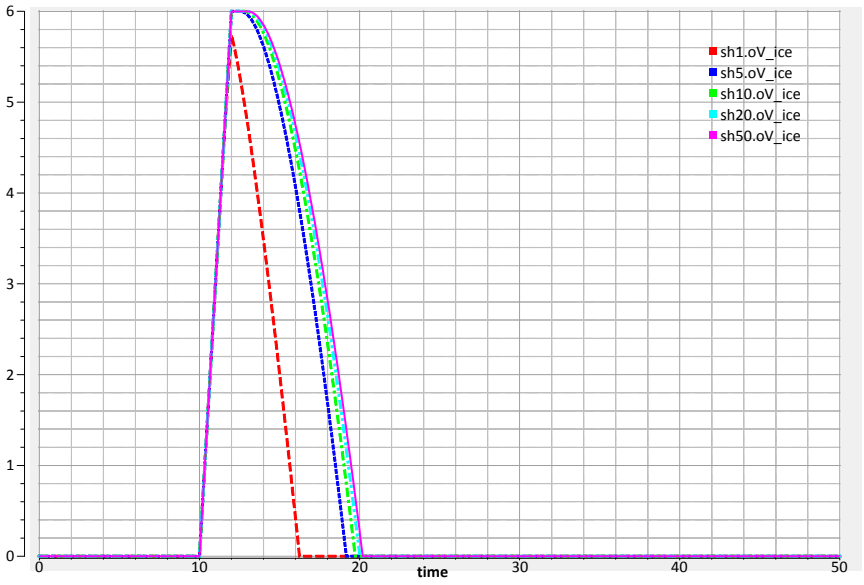

Figure 12: Ice level on surface (`shN.oV_ice`) for various numbers `N` of control volumes in each (distributed) layer.

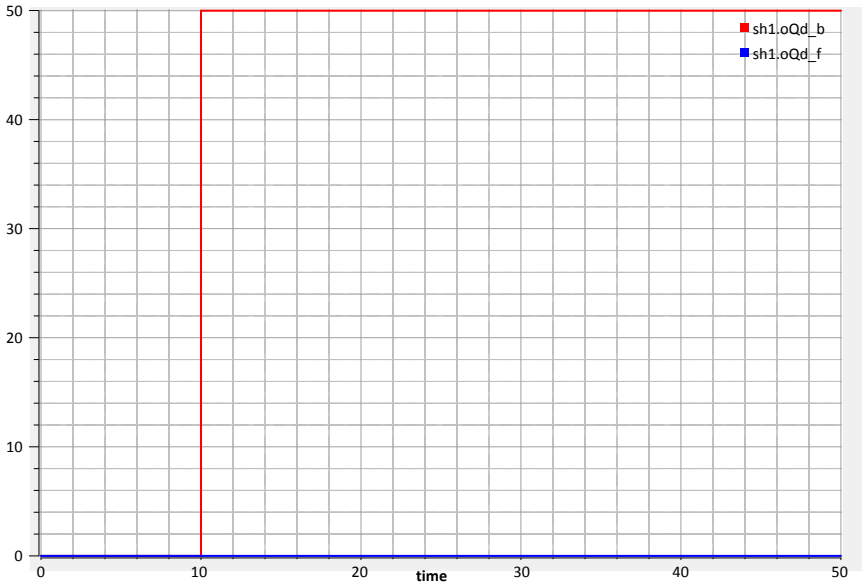

Figure 13: Heating levels, $\dot{Q}''_{\mathrm{b}}$ jumps from $0\,\mathrm{W/\,m^2}$ to $50\,\mathrm{W/\,m^2}$ after $10\,\mathrm{h}$, while $\dot{Q}''_{\mathrm{f}} = 0\,\mathrm{W/\,m^2}$.

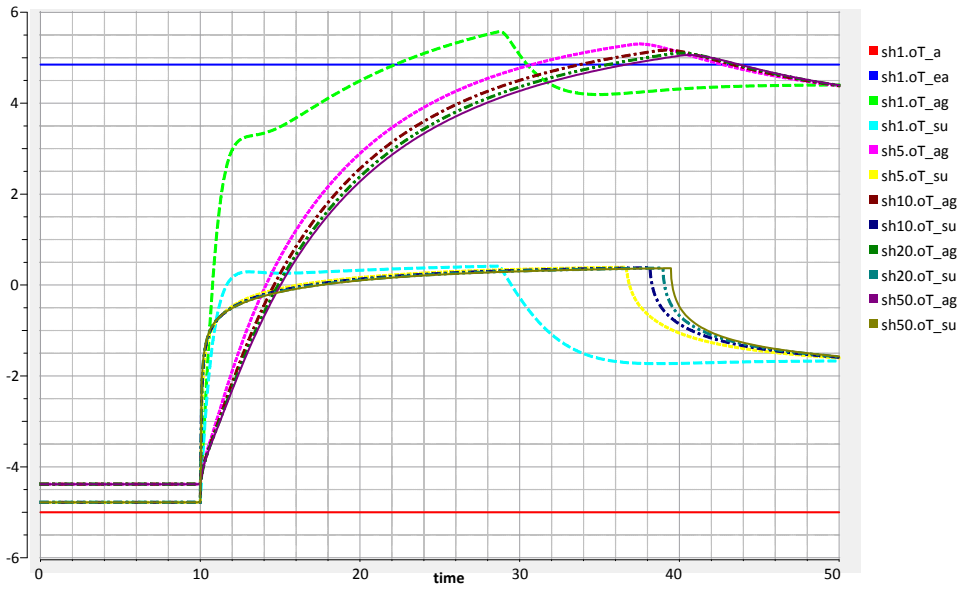

Figure 14: Computed temperature in asphalt layer with glycol pipes (`shN.oT_ag`) and at the surface of the pavement stones (`shN.oT_su`), where `N` specifies the number of control volumes in layers. Atmospheric temperature (`sh1.oT_a`) and earth temperature (`sh1.oT_ea`) are included.

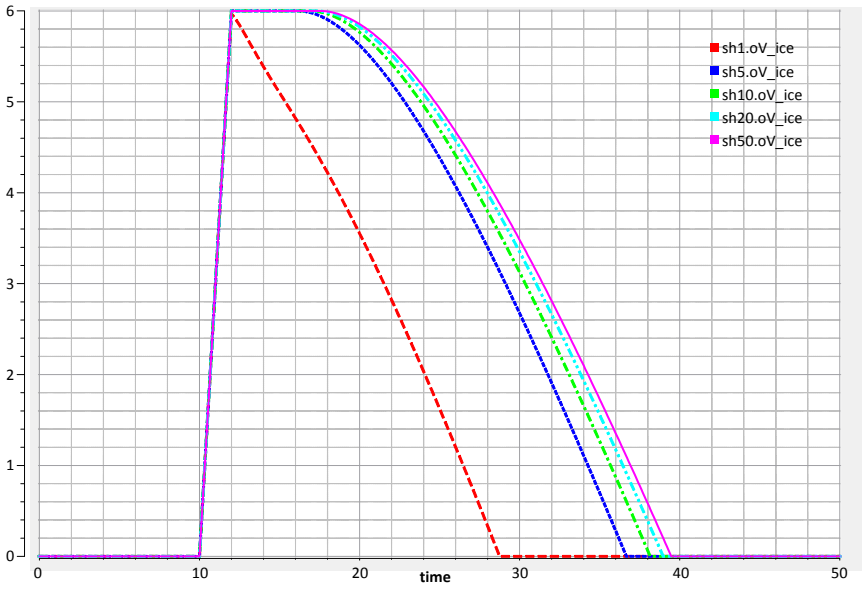

Figure 15: Ice level on surface (`shN.oV_ice`) for various numbers `N` of control volumes in each (distributed) layer.

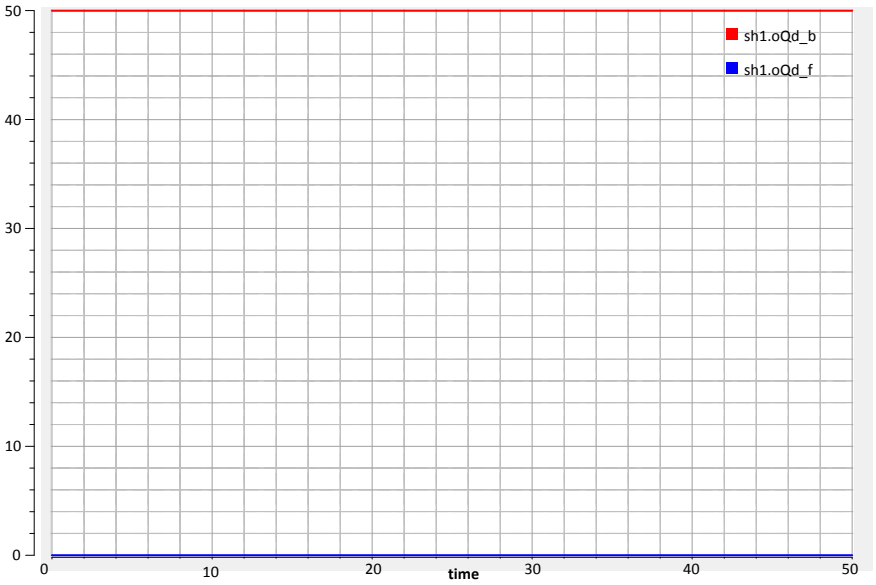

Figure 16: Heating levels, $\dot{Q}''_{\mathrm{b}}$ jumps to $50\,\mathrm{W/\,m^2}$ at $-\infty\,\mathrm{h}$, while $\dot{Q}''_{\mathrm{f}} = 0\,\mathrm{W/\,m^2}$.

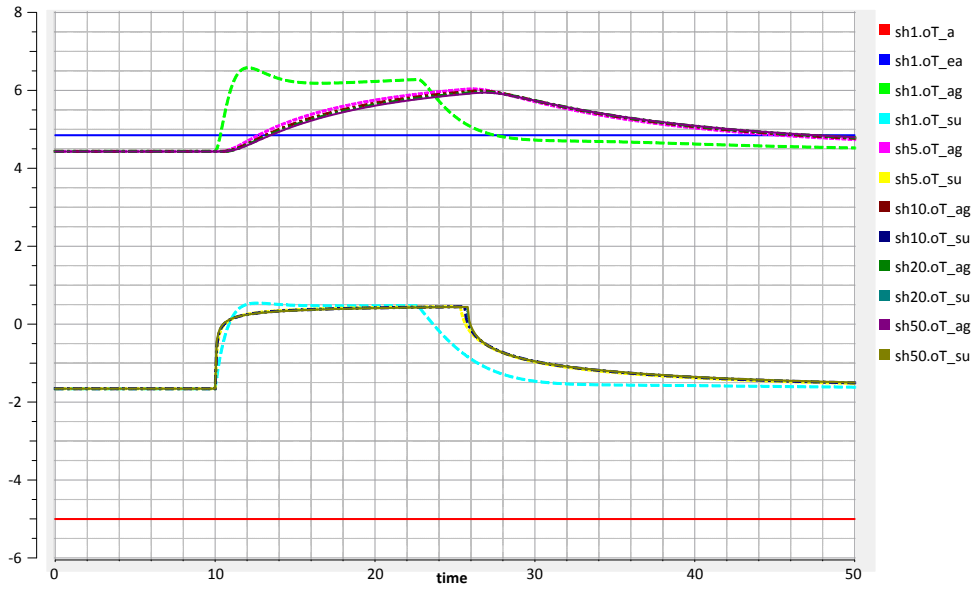

Figure 17: Computed temperature in asphalt layer with glycol pipes (`shN.oT_ag`) and at the surface of the pavement stones (`shN.oT_su`), where `N` specifies the number of control volumes in layers. Atmospheric temperature (`sh1.oT_a`) and earth temperature (`sh1.oT_ea`) are included.

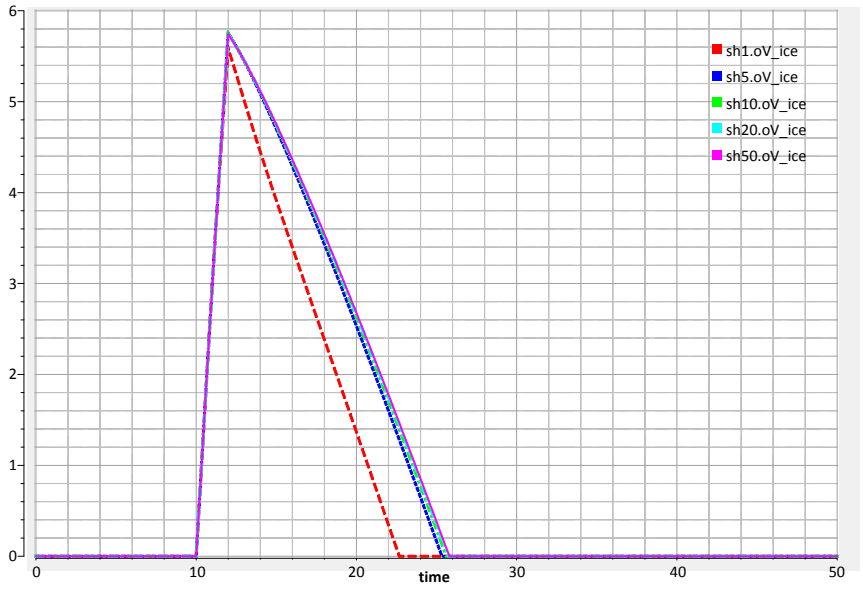

Figure 18: Ice level on surface (`shN.oV_ice`) for various numbers `N` of control volumes in each (distributed) layer.

Figure 18 shows the computed layer of ice on the surface for various numbers of control volumes per layer, $N \in \{1, 5, 10, 20, 50\}$.

The results in this section shows the shortest possible melting time when using only bio fuel constrained by $\dot{Q}''_{\mathrm{b}} \leq 50\,\mathrm{W/\,m^2}$: the case is equivalent to knowing about precipitation infinitely long time in advance.

4.5 Biofuel heating with onset 5 h prior to precipitation

Figure 19 illustrates the heating profile used with onset of biofuel at 5 h.

Figure 20 shows the computed temperature in the upper asphalt layer with glycol pipes, and in the surface of the pavement stones for various numbers of control volumes per layer, $N \in \{1, 5, 10, 20, 50\}$.

Figure 21 shows the computed layer of ice on the surface for various numbers of control volumes per layer, $N \in \{1, 5, 10, 20, 50\}$.

5 Discussion and conclusions

The developed model is based on a number of simplifying assumptions. The main shortcomings are perhaps neglecting the district heating system, and using a simplified surface model with ice only and no inclusion of radiation.

Based on the simulation study, it is reasonable to say that assuming well mixed layers (`N=1`) is too simple for accurate prediction of the surface ice layer, and that one should use at least 5–10 control volumes in the layers. Still, it is possible that a more detailed study allows for fewer control volumes in some layers.

Another conclusion is that using weather forecast of 5 h seems to allow for reduced use of fossil fuel. However, the experiment with "infinite horizon prediciton" shows that there is a potential for using meteorological forecast models. It may be necessary to step up to a bio fuel constraint of $100\,\mathrm{W/\,m^2}$ to gain significant improvement, though, and perhaps to have decent forecast models for more than 5 h.

In order to develop a control system, it is important to extend the model with necessary subsystems related to district heating. Furthermore, it is necessary to think through the costs

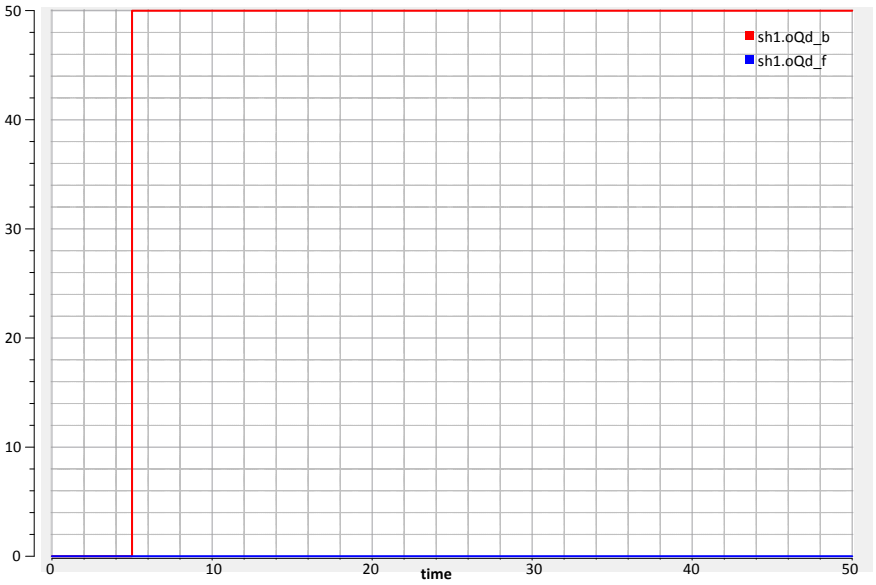

Figure 19: Heating levels, $\dot{Q}''_{\mathrm{b}}$ jumps from $0\,\mathrm{W/\,m^2}$ to $50\,\mathrm{W/\,m^2}$ after $5\,\mathrm{h}$, while $\dot{Q}''_{\mathrm{f}} = 0\,\mathrm{W/\,m^2}$.

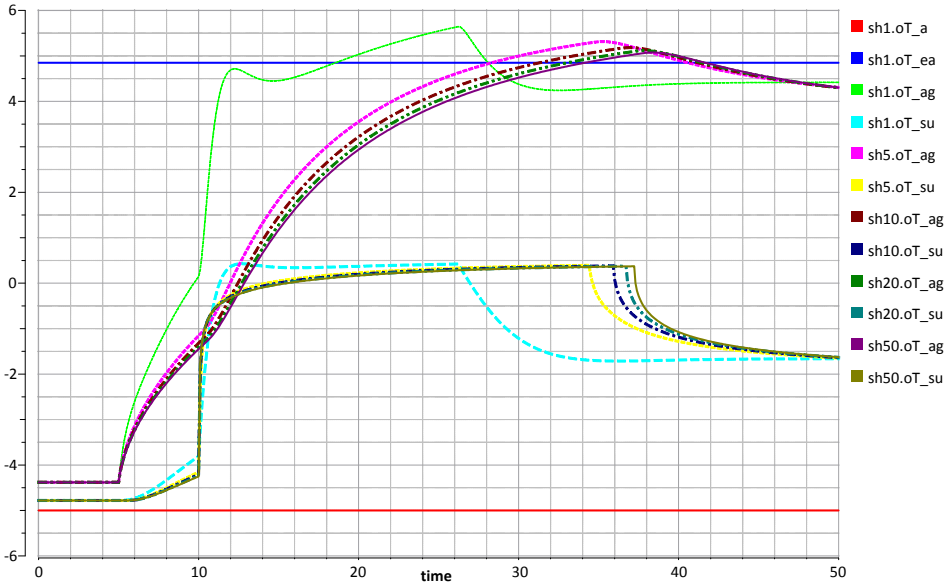

Figure 20: Computed temperature in asphalt layer with glycol pipes (`shN.oT_ag`) and at the surface of the pavement stones (`shN.oT_su`), where `N` specifies the number of control volumes in layers. Atmospheric temperature (`sh1.oT_a`) and earth temperature (`sh1.oT_ea`) are included.

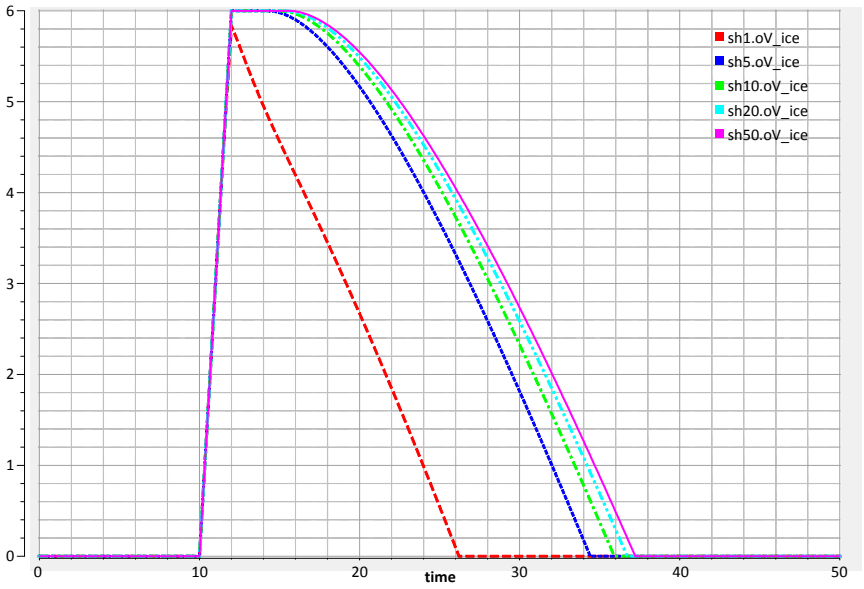

Figure 21: Ice level on surface (`shN.oV_ice`) for various numbers `N` of control volumes in each (distributed) layer.

assosiated with heating vs. the costs associated with allowing for slippy streets: is it less critical with ice coverage during the night? Is the ice really slippy when the outdoor temperature is low (e.g. $-10\,^{\circ}\mathrm{C}$)?

In an attempt to take advantage of weather forecast models, it is important to realize the uncertainty of such models. Thus, a viable control solution will include some form of stochastic model based control/stochastic MPC.

References

[1] Chen, M., Wun, S., Wang, H., and Zhang, J. (2011). "Study of ice and snow melting process on conductive asphalt solar collector". *Solar Energy Materials & Solar Cells*, Vol. 95, pp. 3241 – 3250.

[2] Liu, X. (2005). "Development and Experimental Validation of Simulation of Hydronic Snow Melting Systems for Bridges". PhD thesis, *Faculty of the Graduate College of the Oklahoma State University*.

[3] Lyseng, B. (2012). *Data modelling and simulation of a district heating system*. MSc thesis, *Faculty of Technology of Telemark University College*.

[4] Wang, H., Liu, L., and Chen, Z. (2010). "Experimental investigation of hydronic snow melting process on the inclined pavement". *Cold Regions Science and Technology*, Vol. 63, pp. 44 – 49.